

# Motion Modification Method of Musculoskeletal Humanoids by Human Teaching Using Muscle-Based Compensation Control

Kento Kawaharazuka<sup>1</sup>, Yuya Koga<sup>1</sup>, Manabu Nishiura<sup>1</sup>, Yusuke Omura<sup>1</sup>, Yuki Asano<sup>1</sup>  
Kei Okada<sup>1</sup>, Koji Kawasaki<sup>2</sup>, and Masayuki Inaba<sup>1</sup>

**Abstract**—While musculoskeletal humanoids have the advantages of various biomimetic structures, it is difficult to accurately control the body, which is challenging to model. Although various learning-based control methods have been developed so far, they cannot completely absorb model errors, and recognition errors are also bound to occur. In this paper, we describe a method to modify the movement of the musculoskeletal humanoid by applying external force during the movement, taking advantage of its flexible body. Considering the fact that the joint angles cannot be measured, and that the external force greatly affects the nonlinear elastic element and not the actuator, the modified motion is reproduced by the proposed muscle-based compensation control. This method is applied to a musculoskeletal humanoid, Musashi, and its effectiveness is confirmed.

## I. INTRODUCTION

The musculoskeletal humanoid [1]–[4] has biomimetic advantages such as the redundant muscle arrangement, variable stiffness control using nonlinear elasticity and antagonism, ball joints without singular points, and the flexible spine and fingers. At the same time, the complex and flexible body is difficult to model, and various learning control methods have been developed in order to achieve accurate movements. In [5], joint angles obtained from motion capture and muscle lengths are correlated offline using a neural network. In [6], joint angles obtained from IMU and muscle lengths are correlated using polynomial regression. In [7]–[10], the relationship among joint angles obtained from vision, muscle tensions, and muscle lengths is learned online using a neural network. While these control methods are able to realize the intended joint angles to some extent, because they handle only static models, there are always some errors due to hysteresis, inter-skeletal friction, etc. In response to this problem, some methods have been developed to handle dynamic models, such as [11], but they cannot handle time series information in a large space of joint angles, muscle tensions, and muscle lengths. In addition, recognition errors in the robot are common during motion generation, and even if the robot can move accurately, it may not be able to perform the task accurately.

Therefore, in this study, we change the approach and consider to modify the original motion by applying external force during the motion and then reproduce the modified

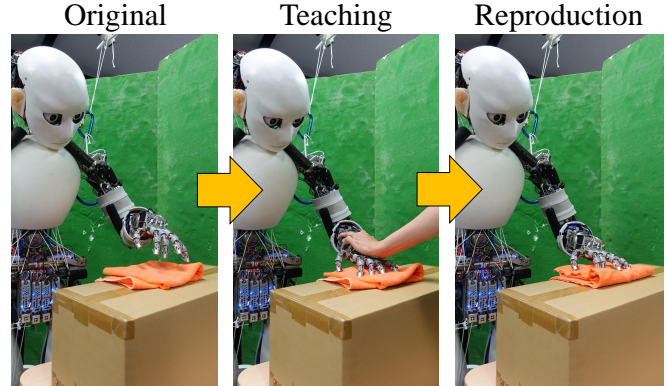


Fig. 1. The overall flow of this study: teaching by humans during the original movement and its reproduction.

motion. Humans can easily change the movements of musculoskeletal humanoids from the outside without any controls due to their flexible bodies, and thus they are considered to have a high affinity with human teaching. At the same time, it is not possible to use the usual teaching methods, such as [12], because the structure of the musculoskeletal humanoid is different from that of the conventional axis-driven humanoid. This is because musculoskeletal humanoids usually do not have sensors to directly measure joint angles due to the presence of ball joints and the complex scapula. Also, nonlinear elastic elements, which ensure the flexibility and variable stiffness control, are provided at the end of the muscle, and the displacement of motion caused by external force is transmitted to the nonlinear elastic elements rather than to the actuator side. Therefore, it is difficult to reproduce the modified motion in the same way with ordinary humanoids. Also, direct teaching methods such as [13] and wearable devices such as [14] have been developed for musculoskeletal humanoids, but these methods do not take into account the fact that the robot is subjected to external force during the motion. In this study, we propose a method to accurately reproduce the modified motion by using muscle tensions during human teaching without using joint angle information and by performing compensatory control at the muscle level (muscle-based compensation control). We apply this method to the musculoskeletal humanoid, Musashi [15], and confirm the effectiveness of this study by performing box wiping and drawing behaviors as well as a basic comparison experiment.

This study is organized as follows. In Section II, the basic musculoskeletal structure and Musculoskeletal AutoEncoder [10], a learning control method developed previously and is used for muscle-based compensation control, are described.

<sup>1</sup> The authors are with the Department of Mechano-Informatics, Graduate School of Information Science and Technology, The University of Tokyo, 7-3-1 Hongo, Bunkyo-ku, Tokyo, 113-8656, Japan. [kawaharazuka, koga, nishiura, omura, asano, k-okada, inaba]@jsk.t.u-tokyo.ac.jp

<sup>2</sup> The author is associated with TOYOTA MOTOR CORPORATION. koji\_kawasaki@mail.toyota.co.jp

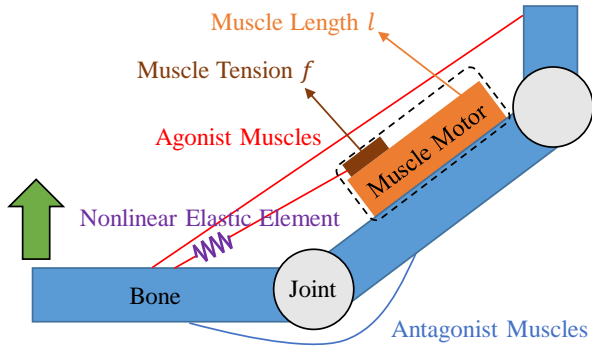


Fig. 2. The basic musculoskeletal structure.

In Section III, the overall flow of this study and muscle tension limiter are described, and then the proposed method of muscle-based compensation control is described. In Section IV, a comparison of the methods described in Section III is presented, and experiments on practical tasks using the proposed method are described. Finally, a discussion is given in Section V and conclusions are presented in Section VI.

## II. MUSCULOSKELETAL HUMANOIDS AND MUSCULOSKELETAL AUTOENCODER

### A. The Basic Structure of Musculoskeletal Humanoids

The basic structure of the musculoskeletal humanoid is shown in Fig. 2. In this study, we mainly handle the musculoskeletal structure in which the muscles are wound by a motor via a pulley. The redundant muscles are arranged antagonistically around joints. The muscles are mainly composed of Dyneema, which is a friction-resistant synthetic fiber, and often have a nonlinear elastic element at the end that enables variable stiffness control. The nonlinear elastic element is elongated by applying muscle tension, and at the same time, Dyneema itself has elasticity, creating the flexibility of the body. Muscle length  $l$  can be measured from an encoder attached to the motor, and muscle tension  $f$  can be measured from a muscle tension measurement unit. Although joint angles  $\theta$  cannot usually be measured as described in Section I, it is possible to measure them in some robots by using a special mechanism [15], [16]. Even when joint angles cannot be directly measured, it is possible to estimate the joint angles of the actual robot using visual sensors, markers attached at the hand, and changes in muscle lengths, as in [7], and this data can be used for learning. However, because of the disadvantage of having to constantly look at the end-effectors, some methods [8]–[10] have been developed to estimate  $\theta$  from  $(f, l)$  by learning the relationship among  $(\theta, f, l)$ .

### B. Musculoskeletal AutoEncoder

We briefly describe Musculoskeletal AutoEncoder (MAE) [10], which is used for the muscle-based compensation control proposed in this study. Note that in this study, the muscle tension  $T$  and the function  $f$  in [10] are converted to  $\mathbf{f}$  and  $\mathbf{h}$ , respectively.

MAE is a neural network representing the relationship among  $(\theta, f, l)$ :  $(\theta, f) \rightarrow l$ ,  $(f, l) \rightarrow \theta$ , and  $(l, \theta) \rightarrow$

$f$ . An AutoEncoder-type network with  $(\theta, f, l)$  and mask value as input, and  $(\theta, f, l)$  as output is updated from the actual robot sensor information. Here, the functions  $h_l$  and  $h_\theta$ , which can be derived from MAE, are defined as  $l = h_l(\theta, f)$ ,  $\theta = h_\theta(l, f)$ . MAE is trained offline and online using the information of actual sensor data. The relationship among  $(\theta, f, l)$  including the information of muscle Jacobian, nonlinear elastic behaviors, etc. is embedded into MAE. By using  $h_\theta$  in MAE, the current estimated joint angle  $\theta^{est}$  can be calculated from the information of  $(f, l)$  (this operation is referred to as EST). Also, by using  $h_l$ , the target muscle length  $l^{ref}$  realizing the target joint angle  $\theta^{ref}$  can be calculated (this operation is referred to as CTRL). It should be noted that it is necessary to calculate the target muscle tension  $f^{ref}$ , which is determined by an iterative calculation using the gravity compensation torque  $\tau$  and the backpropagation method [10]. Also, since the target value  $l^{ref}$  and the measured value  $l$  are different, the muscle stiffness control [17] must be taken into account. Therefore, let  $l^{ref}$  be the value obtained by adding  $l^{comp}$  to  $h_l(\theta^{ref}, f^{ref})$ , as below,

$$l^{comp}(\mathbf{f}) = -(\mathbf{f} - \mathbf{f}^{bias})/K \quad (1)$$

$$l^{ref} = h_l(\theta^{ref}, \mathbf{f}^{ref}) + l^{comp}(\mathbf{f}^{ref}) \quad (2)$$

where  $\mathbf{f}^{bias}$  is the bias term of the muscle stiffness control and  $K$  is the stiffness coefficient.

Note that since MAE represents only static intersensory relationships, it is not possible to estimate completely accurate  $\theta^{est}$  by EST due to hysteresis and friction, and it is not possible to achieve completely accurate  $\theta^{ref}$  by CTRL.

## III. MOTION MODIFICATION USING MUSCLE-BASED COMPENSATION CONTROL

First of all, the overall flow of motion modification by human teaching is described below.

- (a) Making the robot motion (original)
  - (b) Modifying the motion by applying external force while the motion is running (teaching)
  - (c) Reproducing the modified motion (reproduction)
- (a) is usually programmed by humans or generated from the results of recognition and so on. The target joint angle  $\theta_t^{ref}$  is determined, and CTRL calculates the target muscle length  $l_t^{ref}$  and target muscle tension  $f_t^{ref}$ . Here,  $\bullet_t$  refers to the value at the time step  $t$  ( $0 \leq t < T$ ), where  $T$  denotes the length of the motion. In (b), the muscle length  $l_t^{data}$  and muscle tension  $f_t^{data}$  measured during the teaching are accumulated. During the teaching, the original flexibility of the musculoskeletal structure can be used, but it is also possible to increase the effect of the external force by limiting the maximum muscle tension (this will be explained in Section III-A). In (c), the modified motion is reproduced by calculating the muscle length  $\Delta l_t^{ref}$  to be changed from  $l_t^{ref}$  using the obtained  $\{l, f\}_t^{\{ref, data\}}$  and sending  $l_t^{ref} + \Delta l_t^{ref}$  to the actual robot (this will be explained in Section III-B). The methods of reproducing the modified motion for comparison experiments is summarized in Section III-C.

### A. Muscle Tension Limiter

For each muscle, the muscle tension limiter calculates the degree of muscle length relaxation  $\Delta l_{e,t}^{ref}$  according to the current muscle tension as below, and sends  $l_t^{ref} + \Delta l_{e,t}^{ref}$  to the actual robot.

$$\begin{aligned} & \text{if } f_t > f^{max} \\ & \quad \Delta l_{e,t}^{ref} = \Delta l_{e,t-1}^{ref} + \min(C_{gain}d - \Delta l_{e,t-1}^{ref}, C_{plus}d) \\ & \text{else} \\ & \quad \Delta l_{e,t}^{ref} = \Delta l_{e,t-1}^{ref} + \max(0 - \Delta l_{e,t-1}^{ref}, -C_{minus}d) \\ & d_t = |f_t - f^{max}| \end{aligned} \quad (3)$$

where  $f^{max}$  is the threshold of the muscle tension  $f$  that begins to relax the muscle length,  $|\bullet|$  is the absolute value,  $C_{\{minus,plus\}}$  is the coefficient that determines the amount of muscle length change in one step in the negative or positive direction, and  $C_{gain}$  is the coefficient that determines the maximum amount of relaxation. In other words, the muscle is relaxed and tensed so that the muscle tension does not exceed the maximum value while limiting  $\Delta l_{e,t}^{ref}$  by  $C_{minus}d_t$  and  $C_{plus}d_t$ . When external force is applied, the muscle tension increases, and the muscle is stretched by the amount over  $f^{thre}$ , so that the motion can be modified more easily and significantly by teaching. In this study, we set  $C_{minus} = 0.001$  [mm/N],  $C_{plus} = 0.003$  [mm/N], and  $C_{gain} = 2.0$  [mm/N], and this control is performed with a period of 8 msec.  $f^{thre}$  is varied according to the experiment.

### B. Muscle-based Compensation Control

For the ordinary axis-driven humanoid, we only need to take the joint angle  $\theta_t^{data}$  of the modified motion and send it to the actual robot as the target value  $\theta_t^{ref}$ . However, such a method is impractical because musculoskeletal humanoids cannot measure the joint angle  $\theta_t^{data}$  directly, as described in Section I. The joint angle  $\theta_t^{est}$  estimated by EST can be used, but the error of MAE accumulates due to the two steps of estimation by EST and calculation by CTRL (the comparison experiment will be performed in the experimental section). On the other hand, we can take the muscle length  $l_t^{data}$  of the modified behavior and send it to the actual robot as the target value  $l_t^{ref}$ . However, as described in Section II-A, the effect of external force appears not on  $l_t^{data}$  but on the elongation of the hardware of the nonlinear elastic element or the muscle wire itself. Therefore, even if the measured muscle length is sent, it is not possible to reflect the external force well. In this study, we propose to calculate a term  $\Delta l_t^{ref}$  that compensates muscle length at the muscle level based on the information obtained from MAE described in Section II-B, and reproduce the modified motion by adding it to  $l_t^{ref}$ .

We propose a method to reproduce the modified motion by adding the following terms (A)-(C) to the original target muscle length  $l_t^{ref}$ . These are (A)  $\Delta l_{e,t}^{ref}$ , the elongation due to the muscle tension limiter in Section III-A, (B)  $\Delta l_{h,t}^{ref}$ , the elongation due to the hardware elasticity of the nonlinear elastic element or the muscle wire itself, and (C)  $\Delta l_{s,t}^{ref}$ , the elongation due to the software of the muscle stiffness control.

(A) is very simple: add  $\Delta l_{e,t}^{ref}$  in Eq. 3 to  $l_t^{ref}$ .

(B) calculates the muscle elongation term due to the hardware using MAE as below.

$$\begin{aligned} \theta_t^{est} &= \mathbf{h}_\theta(\mathbf{f}_t^{data}, \mathbf{l}_t^{data}) \\ \Delta l_{h,t}^{ref} &= -(\mathbf{h}_l(\theta_t^{est}, \mathbf{f}_t^{data}) - \mathbf{h}_l(\theta_t^{est}, \mathbf{f}_t^{ref})) \end{aligned} \quad (4)$$

$\Delta l_{h,t}^{ref}$  indicates the extent to which muscle length as hardware changes when changing the muscle tension at the same joint angle. This calculation takes advantage of the fact that (i) the muscle tension required for gravity compensation and (ii) the hardware elasticity of the muscle do not change significantly between  $\theta^{ref}$  and  $\theta^{data}$ . Although the muscle tension is increased by the external force at the time of teaching, by assuming (i), we make sure that the muscle tension, when the modified motion is reproduced, is close to that of the original  $\mathbf{f}^{ref}$ . Also, the assumption in (ii) simplifies the equation of Eq. 4. Indeed,  $\mathbf{h}_l(\theta, \mathbf{f})$  can be decomposed into  $\mathbf{h}_1(\theta)$  and  $\mathbf{h}_2(\theta, \mathbf{f})$ , as in [8].  $\mathbf{h}_1$  represents the muscle length at  $\theta$  when  $\mathbf{f} = \mathbf{0}$ , and  $\mathbf{h}_2$  represents the compensation term for the hardware elongation of the muscle length to keep  $\theta$  (always negative). Therefore, by substituting the same  $\theta_t^{est}$  for  $\theta$ ,  $\mathbf{h}_1$  is canceled out in Eq. 4, and the change in the compensation term for the hardware elongation of the muscle around  $\theta_t^{est}$ ,  $\mathbf{h}_2(\theta_t^{est}, \mathbf{f}_t^{data}) - \mathbf{h}_2(\theta_t^{est}, \mathbf{f}_t^{ref})$ , which is only the change in the hardware elongation of the muscle, can be calculated. Since this is a compensation term and a negative value, it is necessary to reverse the sign of the term.

(C) calculates the software muscle elongation from the equation of the muscle stiffness control in Eq. 1 as below.

$$\Delta l_{s,t}^{ref} = -(l^{comp}(\mathbf{f}_t^{data}) - l^{comp}(\mathbf{f}_t^{ref})) \quad (5)$$

As in (B), we use the assumption of (i) and calculate the software elongation of muscles. Since this is also a compensation term and a negative value, it is necessary to reverse the sign of the term.

Finally, (a)-(c) in Section III represent an interesting relationship when diagrammed as shown in Fig. 3. Between the original and teaching, with  $l^{ref}$  in common, there is a difference regarding  $\theta^{ref}$  and  $\mathbf{f}^{ref}$  depending on the external force. Also, between the teaching and reproduction, with  $\theta^{data}$  in common, there is a difference regarding  $\mathbf{f}^{ref}$  and  $l^{ref}$ . In this study, we assume (i), that the muscle tension between the original and reproduction is not significantly different. Therefore, we can construct a structure in which one value is fixed between each operation, and the relationship between the other two values is different. Normally,  $\theta^{data}$  and  $\mathbf{f}^{ref}$  are used to obtain  $l^{ref} + \Delta l$  in reproduction (joint-based), but in this study,  $l^{ref} + \Delta l$  is obtained under the conditions that  $\theta^{data}$  is not obtained and  $\mathbf{f}^{data}$  is known (muscle-based). It is possible to understand this scheme from the relationship of Fig. 3.

In this study, the time stamp  $t$  is an interval of 0.2 seconds.

### C. Comparison of Controls Reproducing the Modified Motion

The methods to be evaluated in the comparison experiment of this study are listed below.

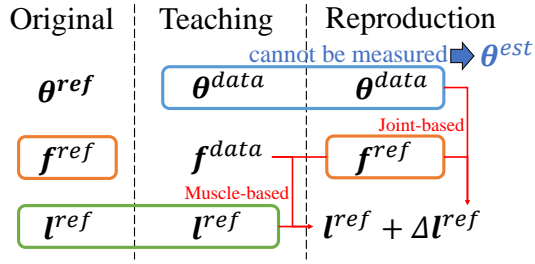


Fig. 3. The relationship of  $(\theta, f, l)$  among original, teaching, and reproduction.

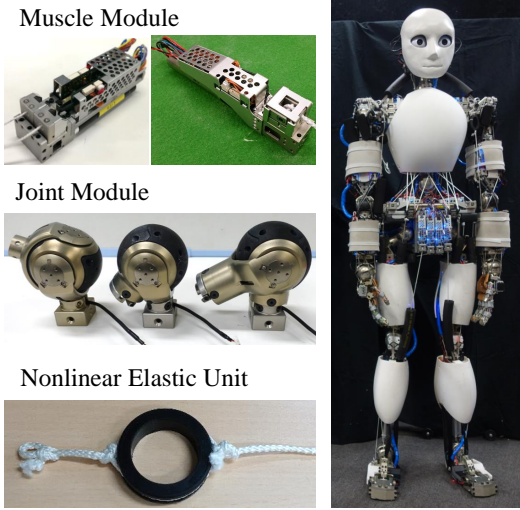


Fig. 4. Experimental setup.

- ALL:  $\Delta l_t^{ref} = \Delta l_{e,t}^{ref} + \Delta l_{h,t}^{ref} + \Delta l_{s,t}^{ref}$
- W-HS:  $\Delta l_t^{ref} = \Delta l_{h,t}^{ref} + \Delta l_{s,t}^{ref}$
- W-ES:  $\Delta l_t^{ref} = \Delta l_{e,t}^{ref} + \Delta l_{s,t}^{ref}$
- W-HE:  $\Delta l_t^{ref} = \Delta l_{h,t}^{ref} + \Delta l_{e,t}^{ref}$
- W-H:  $\Delta l_t^{ref} = \Delta l_{h,t}^{ref}$
- W-E:  $\Delta l_t^{ref} = \Delta l_{e,t}^{ref}$
- W-S:  $\Delta l_t^{ref} = \Delta l_{s,t}^{ref}$
- NONE:  $\Delta l_t^{ref} = 0$
- THETA: A method calculating  $\theta_t^{est}$  by EST and calculating  $l_t^{ref}$  to realize  $\theta_t^{est}$ .

#### IV. EXPERIMENTS

##### A. Experimental Setup

In this study, we use the musculoskeletal humanoid Musashi [15]. The right figure of Fig. 4 is Musashi, and the left figures show each component that constitutes it. A nonlinear elastic element using Grommet is arranged at the end of the muscle wire, Dyneema. In this study, we mainly used three degrees of freedom (DOFs) of the shoulder and two DOFs of the elbow. Unlike ordinary musculoskeletal humanoids, Musashi is equipped with a mechanism to directly measure the joint angle for experimental evaluation. We do not use this value in our experiments, but we use it to evaluate whether or not the modified motion is accurately reproduced.

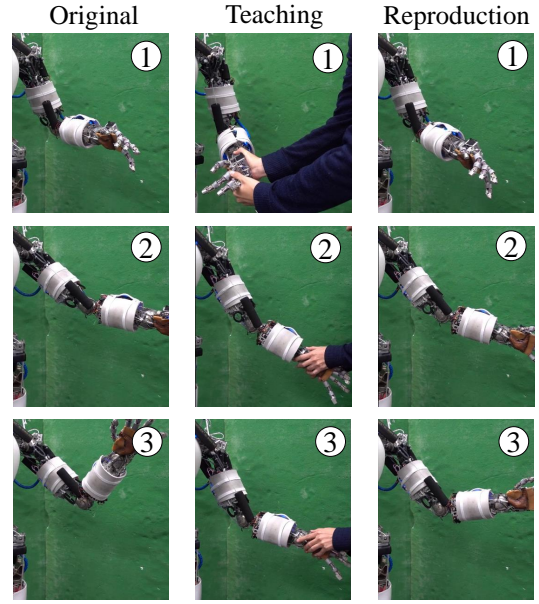


Fig. 5. The procedure in the comparison experiment of motion modification methods.

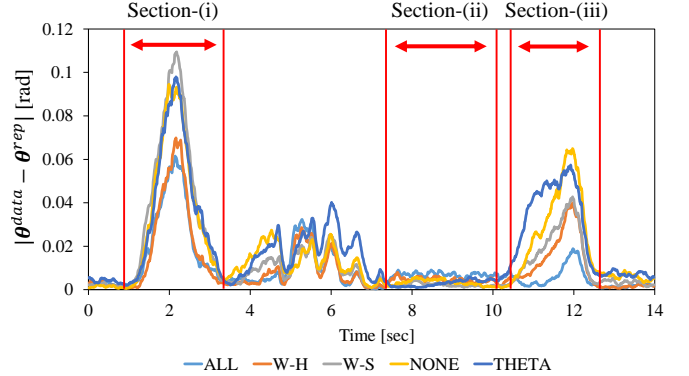


Fig. 6. Transition of  $|\theta_t^{data} - \theta_t^{rep}|$  in the comparison experiment without muscle tension limiter.

##### B. Comparison Experiment

In this experiment, we compare the performance of the methods presented in Section III-C. We generate the basic motion as shown in the left figures of Fig. 5. Then, we modify it by applying external force as shown in the middle figures. Finally, the modified behavior is reproduced by the respective methods of Section III-C as shown in the right figures. Then, we compare the joint angle  $\theta_t^{data}$  during teaching in the middle figures and the joint angle  $\theta_t^{rep}$  during the reproduction in the right figures.  $E$  expresses the average of the total time of  $|\theta_t^{data} - \theta_t^{rep}|$ . Fig. 5 is the experiment in the second half of this section, and reproduction shows the case of using the method ALL. In this experiment, the base link was moved by external force, so the comparison using the images is only a reference.

First, the transition of  $|\theta_t^{data} - \theta_t^{rep}|$  without muscle tension limiter of Section III-A is shown in Fig. 6. We focus on the intervals from Section-(i) to Section-(iii) in the 14

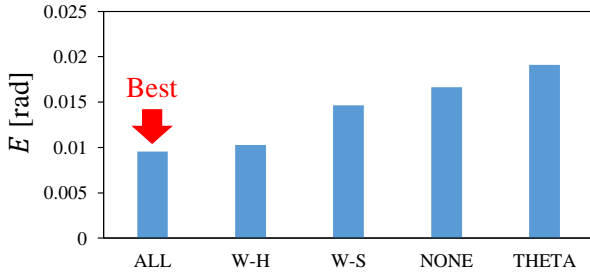


Fig. 7. Comparison of evaluation value  $E$  in the comparison experiment without muscle tension limiter.

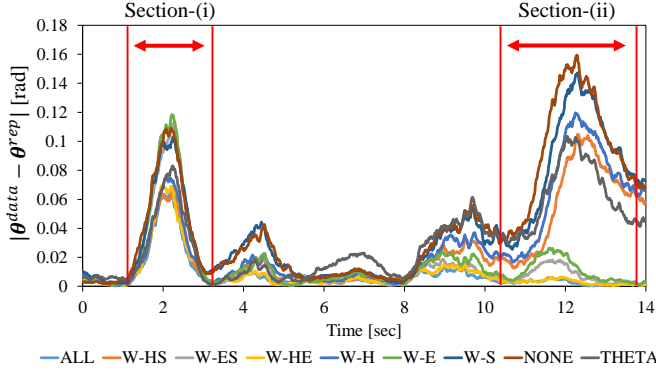


Fig. 8. Transition of  $|\theta_t^{data} - \theta_t^{rep}|$  in the comparison experiment with muscle tension limiter.

second operation. In Section-(i), the accuracy was  $ALL \simeq W-H > W-S \simeq NONE \simeq THETA$ . In Section-(ii), the accuracy of ALL was the worst, although they were almost the same in each case. In Section-(iii), the accuracy was  $ALL > W-H \simeq W-S > NONE \simeq THETA$ . In other words, in Section-(i), the effect of  $\Delta l_{h,t}^{ref}$  was large, while the effect of  $\Delta l_{s,t}^{ref}$  was small. Therefore,  $ALL \simeq W-H$  and, conversely,  $W-S \simeq NONE$ . THETA was almost the same as NONE, and its accuracy was low. In Section-(iii), it could be seen that the effects of  $\Delta l_{h,t}^{ref}$  and  $\Delta l_{s,t}^{ref}$  were almost the same. The best performance was obtained by considering the two influences of software and hardware, realized in ALL. On the other hand, for Section-(ii), the accuracy of ALL was the worst. When  $|\theta_t^{data} - \theta_t^{rep}|$  is low overall without large external force, it is considered that errors in MAE and muscle tension measurement dominate. The comparison of the values of  $E$  for each of these methods is shown in Fig. 7. The accuracy results are shown as  $ALL > W-H > W-S > NONE > THETA$ , indicating that the error of ALL is about half that of THETA.

Next, the transition of  $|\theta_t^{data} - \theta_t^{rep}|$  in the case of using muscle tension limiter in Section III-A is shown in Fig. 8. In this experiment, we set  $f^{thre} = 100$  [N]. We similarly focus on Section-(i) and Section-(ii). In Section-(i), the accuracy was  $ALL \simeq W-HS \simeq W-H \simeq W-H \simeq THETA > W-ES \simeq W-E \simeq W-S \simeq NONE$ . In Section-(ii), the accuracy was  $ALL \simeq W-ES \simeq W-HE \simeq W-E > W-HS \simeq W-H \simeq W-S \simeq NONE \simeq THETA$ . In other words, in Section-(i), the effect of  $\Delta l_{h,t}^{ref}$  was the largest, whereas in Section-(ii), the effect of

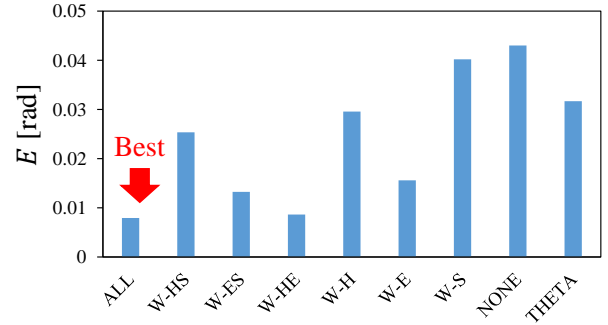


Fig. 9. Comparison of evaluation value  $E$  in the comparison experiment with muscle tension limiter.

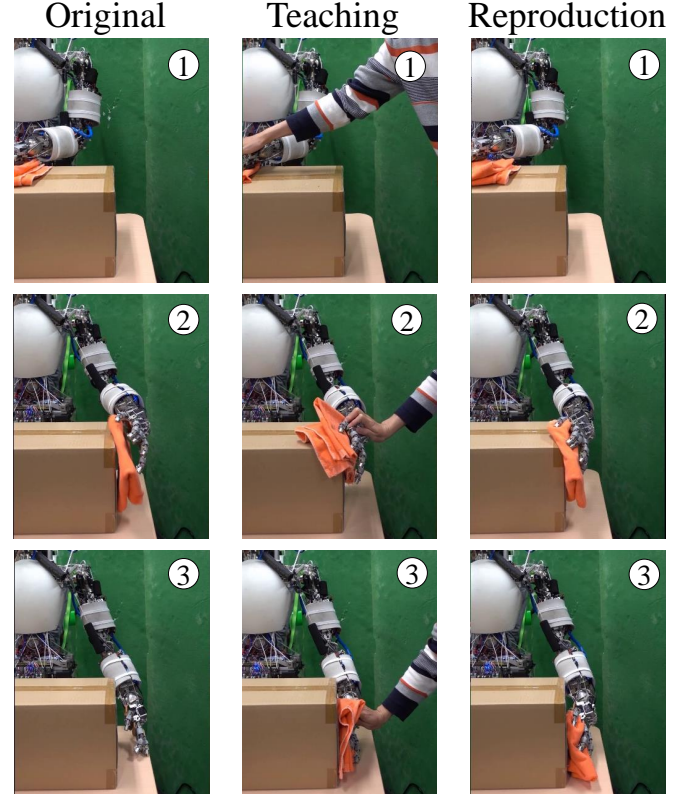


Fig. 10. Box wiping experiment.

$\Delta l_{e,t}^{ref}$  was the largest. Although THETA was good at some intervals, it was not so good when viewed as a whole. A comparison of the values of  $E$  for each of these methods is shown in Fig. 9. The accuracy was  $ALL > W-HE > W-ES > W-E > W-HS > THETA > W-S > NONE$ , indicating that the error of ALL was less than one third of that of THETA. It could also be seen that the overall degree of influence was  $\Delta l_{e,t}^{ref} > \Delta l_{h,t}^{ref} > \Delta l_{s,t}^{ref}$ . The error of THETA was not much different from that of W-H.

### C. Box Wiping Experiment

Wiping the two planes of a box is performed using the method of this study. In this experiment, the muscle tension limiter is not running. The flow is shown in Fig. 10. First,

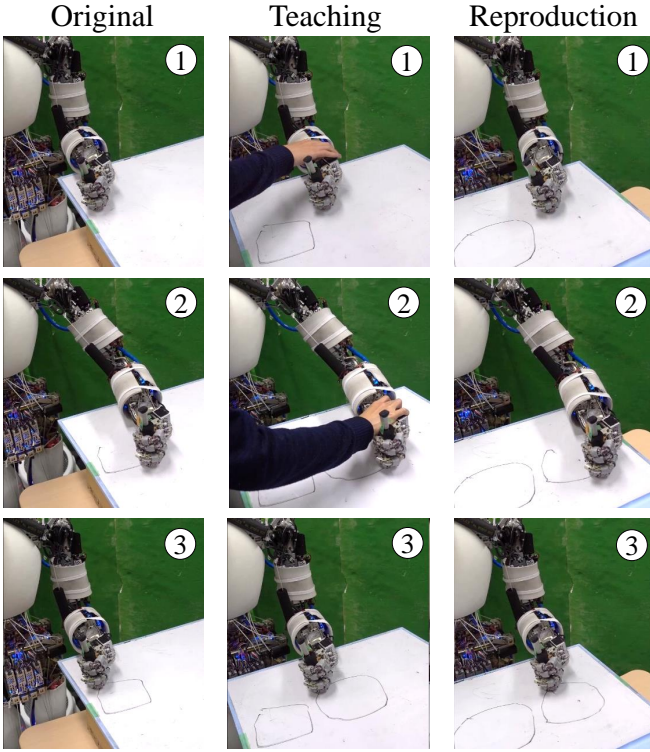


Fig. 11. Drawing experiment.

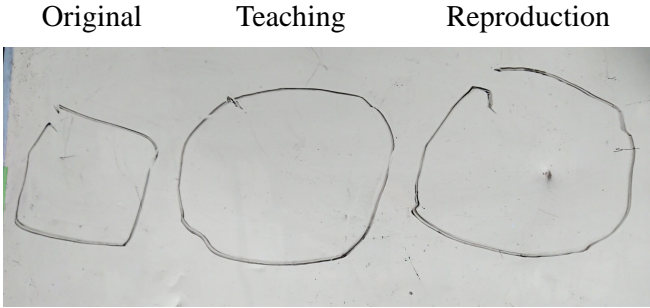


Fig. 12. The result of drawn objects.

we generate the motion of wiping the box using inverse kinematics. However, we can see that the hand moves away from the box when wiping the vertical plane due to the error of the joint angle, and the cloth falls out of the hand. Next, we modify the motion so that the side of the box can be wiped correctly by applying external force during the motion. Finally, when the modified motion is reproduced using ALL without human guidance, we confirmed that the cloth could be wiped down to the end by pressing a hand on the side of the box.

#### D. Drawing Experiment

We modify the motion of drawing a square to that of drawing a circle using our method. In this experiment, the muscle tension limiter is running as  $f^{thre} = 200$  [N]. The flow of the experiment is shown in Fig. 11. First, we generate

the motion of drawing a square by using inverse kinematics. Next, we guide it from the outside and change the motion to the drawing of a circle. Finally, the modified motion is reproduced using our method, ALL. The final result is shown in Fig. 12. we can see that the initial result is a rectangle, but the teaching result is a circle, and the reproduced result is a similar one.

#### V. DISCUSSION

In the comparison experiment, various findings were obtained regarding the effects of the terms  $\Delta l_{e,t}^{ref}$ ,  $\Delta l_{h,t}^{ref}$ , and  $\Delta l_{s,t}^{ref}$ . The effect of  $\Delta l_{e,t}^{ref}$  disappears when muscle tension limiter is not used, and there are intervals in which  $\Delta l_{h,t}^{ref}$  dominates, and intervals in which the effect of  $\Delta l_{s,t}^{ref}$  and  $\Delta l_{h,t}^{ref}$  are comparable. This corresponds to the fact that there are intervals in which the effect of hardware is large and those in which the effect of hardware is small and is comparable to that of muscle elongation caused by software. Because the nonlinear elasticity of the nonlinear elastic unit degrades over time, the hardware elongation due to muscle tension may become small. In addition, in the case of a muscle with high muscle tension from the beginning, the hardware elongation of the muscle due to muscle tension decreases due to its nonlinearity, and it is less susceptible to the effect of external force. The validity of this method is demonstrated by the fact that ALL, which can take into account the effects of the hardware and software, gives the best result. At the same time, it is shown that the accuracy of ALL is the worst in the interval where the influence of external force is small, and that the method is able to take into account various factors and at the same time is susceptible to errors. Also, ALL is not able to reproduce the taught joint angle completely accurately, mainly because the assumption of MAE that the target muscle tension is completely achieved by the actual robot does not necessarily hold. Since MAE can only consider static factors, errors are caused by the effects of friction and hysteresis.

In the case of using muscle tension limiter, the effects of  $\Delta l_{e,t}^{ref}$  and  $\Delta l_{h,t}^{ref}$  are found to be dominant. The degree of each influence varies with the intervals. When a strong external force is applied while the original muscle tension is high, the muscle tension is limited by  $f^{thre}$  and  $\Delta l_{e,t}^{ref}$  becomes dominant. Conversely, if the original muscle tension is low,  $\Delta l_{e,t}^{ref}$  is not reached even when external force is applied, and  $\Delta l_{h,t}^{ref}$  becomes dominant. Taken as a whole, the degree of influence is  $\Delta l_{e,t}^{ref} > \Delta l_{h,t}^{ref} > \Delta l_{s,t}^{ref}$ . As a whole, ALL, which can consider all elements, shows the best accuracy, demonstrating the validity of our method. Through the comparison experiments, we found that the accuracy of THETA is low and that it is not suitable to reproduce the modified motion of musculoskeletal humanoids directly through the estimated joint angles.

In the box wiping and drawing experiments, the practical effectiveness of this study is shown. It should be noted that in the drawing experiment, we were not able to draw well when we applied this method to all the muscles. Due to the large

friction in the elbow muscles, the error of MAE was large, the hand was lifted up when the movement was reproduced, and the pen did not touch the whiteboard. However, when we performed the experiment without applying this method to two muscles of the elbow, we were able to reproduce the taught movements accurately. In other words, the method is sensitive to the error of MAE, i.e., the estimated value of nonlinear elasticity, and we need to train it so that it can estimate the value firmly.

Finally, the scope of this study is discussed. In this study, we mainly make the robot move by specifying joint angles directly or by generating simple motions with inverse kinematics and then modifying the motions. In the same way, we can slightly modify the motion of the robot generated by human teaching with a teaching device. Also, because musculoskeletal humanoids cannot measure joint angles, it is difficult to initialize the origin of muscle length. This method can be used to modify some of the subtle changes in the behavior when initializing it again. Although our method is currently designed to reproduce a single demonstration from humans, the motion may be learned from the data obtained by performing the demonstration many times in the future. Also, the method of incrementally modifying the behavior is expected to be developed.

## VI. CONCLUSION

In this study, a method to modify the motion of the musculoskeletal humanoid by human teaching is discussed, taking advantage of the flexible body characteristics, although it is difficult to model. We developed a new method for reproduction of the modified motion by muscle-based compensation control, which takes into account the fact that joint angles cannot be measured and the influence of muscle tension is propagated to the hardware elasticity side of the muscle, which is different from the axis-driven type. Using information obtained from Musculoskeletal AutoEncoder, we confirmed through experiments that the hardware elasticity can be estimated and the modified motion can be reproduced accurately. Although the effects of muscle tension limiter, hardware elongation, and software elongation are different for each situation, the accuracy is the best when all of them are considered.

In the future, we would like to investigate a method for musculoskeletal humanoids to cooperate with humans.

## REFERENCES

- [1] Y. Nakanishi, S. Ohta, T. Shirai, Y. Asano, T. Kozuki, Y. Kakehashi, H. Mizoguchi, T. Kurotobi, Y. Motegi, K. Sasabuchi, J. Urata, K. Okada, I. Mizuuchi, and M. Inaba, "Design Approach of Biologically-Inspired Musculoskeletal Humanoids," *International Journal of Advanced Robotic Systems*, vol. 10, no. 4, pp. 216–228, 2013.
- [2] S. Wittmeier, C. Alessandro, N. Bascarevic, K. Dalamagkidis, D. Devereux, A. Diamond, M. Jäntschi, K. Jovanovic, R. Knight, H. G. Marques, P. Milosavljevic, B. Mitra, B. Svetozarevic, V. Potkonjak, R. Pfeifer, A. Knoll, and O. Holland, "Toward Anthropomorphic Robotics: Development, Simulation, and Control of a Musculoskeletal Torso," *Artificial Life*, vol. 19, no. 1, pp. 171–193, 2013.
- [3] M. Jäntschi, S. Wittmeier, K. Dalamagkidis, A. Panos, F. Volkart, and A. Knoll, "Anthrob - A Printed Anthropomorphic Robot," in *Proceedings of the 2013 IEEE-RAS International Conference on Humanoid Robots*, 2013, pp. 342–347.
- [4] Y. Asano, T. Kozuki, S. Ookubo, M. Kawamura, S. Nakashima, T. Katayama, Y. Iori, H. Toshinori, K. Kawaharazuka, S. Makino, Y. Kakiuchi, K. Okada, and M. Inaba, "Human Mimetic Musculoskeletal Humanoid Kengoro toward Real World Physically Interactive Actions," in *Proceedings of the 2016 IEEE-RAS International Conference on Humanoid Robots*, 2016, pp. 876–883.
- [5] I. Mizuuchi, Y. Nakanishi, T. Yoshikai, M. Inaba, H. Inoue, and O. Khatib, "Body Information Acquisition System of Redundant Musculo-Skeletal Humanoid," in *Experimental Robotics IX*, 2006, pp. 249–258.
- [6] S. Ookubo, Y. Asano, T. Kozuki, T. Shirai, K. Okada, and M. Inaba, "Learning Nonlinear Muscle-Joint State Mapping Toward Geometric Model-Free Tendon Driven Musculoskeletal Robots," in *Proceedings of the 2015 IEEE-RAS International Conference on Humanoid Robots*, 2015, pp. 765–770.
- [7] K. Kawaharazuka, S. Makino, M. Kawamura, Y. Asano, K. Okada, and M. Inaba, "Online Learning of Joint-Muscle Mapping using Vision in Tendon-driven Musculoskeletal Humanoids," *IEEE Robotics and Automation Letters*, vol. 3, no. 2, pp. 772–779, 2018.
- [8] K. Kawaharazuka, S. Makino, M. Kawamura, A. Fujii, Y. Asano, K. Okada, and M. Inaba, "Online Self-body Image Acquisition Considering Changes in Muscle Routes Caused by Softness of Body Tissue for Tendon-driven Musculoskeletal Humanoids," in *Proceedings of the 2018 IEEE/RSJ International Conference on Intelligent Robots and Systems*, 2018, pp. 1711–1717.
- [9] K. Kawaharazuka, K. Tsuzuki, S. Makino, M. Onitsuka, Y. Asano, K. Okada, K. Kawasaki, and M. Inaba, "Long-time Self-body Image Acquisition and its Application to the Control of Musculoskeletal Structures," *IEEE Robotics and Automation Letters*, vol. 4, no. 3, pp. 2965–2972, 2019.
- [10] K. Kawaharazuka, K. Tsuzuki, M. Onitsuka, Y. Asano, K. Okada, K. Kawasaki, and M. Inaba, "Musculoskeletal AutoEncoder: A Unified Online Acquisition Method of Intersensory Networks for State Estimation, Control, and Simulation of Musculoskeletal Humanoids," *IEEE Robotics and Automation Letters*, vol. 5, no. 2, pp. 2411–2418, 2020.
- [11] K. Kawaharazuka, K. Tsuzuki, S. Makino, M. Onitsuka, K. Shinjo, Y. Asano, K. Okada, K. Kawasaki, and M. Inaba, "Task-specific Self-body Controller Acquisition by Musculoskeletal Humanoids: Application to Pedal Control in Autonomous Driving," in *Proceedings of the 2019 IEEE/RSJ International Conference on Intelligent Robots and Systems*, 2019, pp. 813–818.
- [12] A. Billard, S. Calinon, R. Dillmann, and S. Schaal, "Survey: Robot programming by demonstration," *Handbook of robotics*, 2008.
- [13] I. Mizuuchi, R. Tajima, T. Yoshikai, D. Sato, K. Nagashima, M. Inaba, Y. Kuniyoshi, and H. Inoue, "The Design and Control of the Flexible Spine of a Fully Tendon-Driven Humanoid 'Kenta'," in *Proceedings of the 2004 IEEE/RSJ International Conference on Intelligent Robots and Systems*, 2004, pp. 1192–1197.
- [14] T. Kurotobi, T. Shirai, Y. Motegi, Y. Nakanishi, K. Okada, and M. Inaba, "Controlling tendon driven humanoids with a wearable device with Direct-Mapping Method," in *Proceedings of the 21st IEEE International Symposium on Robot and Human Interactive Communication*, 2012, pp. 437–442.
- [15] K. Kawaharazuka, S. Makino, K. Tsuzuki, M. Onitsuka, Y. Nagamatsu, K. Shinjo, T. Makabe, Y. Asano, K. Okada, K. Kawasaki, and M. Inaba, "Component Modularized Design of Musculoskeletal Humanoid Platform Musashi to Investigate Learning Control Systems," in *Proceedings of the 2019 IEEE/RSJ International Conference on Intelligent Robots and Systems*, 2019, pp. 7294–7301.
- [16] J. Urata, Y. Nakanishi, A. Miyadera, I. Mizuuchi, T. Yoshikai, and M. Inaba, "A Three-Dimensional Angle Sensor for a Spherical Joint Using a Micro Camera," in *Proceedings of the 2006 IEEE International Conference on Robotics and Automation*, 2006, pp. 4428–4430.
- [17] T. Shirai, J. Urata, Y. Nakanishi, K. Okada, and M. Inaba, "Whole body adapting behavior with muscle level stiffness control of tendon-driven multi-joint robot," in *Proceedings of the 2011 IEEE International Conference on Robotics and Biomimetics*, 2011, pp. 2229–2234.